INTRODUCTION

I. Earth-like Exoplanets

- Goal of NASA's Kepler Mission: find terrestrial planets with 2 major factors in consideration:[1]
  1. **Earth-mass exoplanet**→ similar composition.
  2. **Habitable Zone (HZ)** → range of distance from the star; ensure the liquid form of water. [2][3]
- To date, Candidate exoplanets: **4,496**; Confirmed: **2,341**; Confirmed less than twice Earth-size: **30**
- Ways of detection: **radial velocity (RV),** transit, microlensing, direct imaging (Table 1) [4]

How to detect exoplanets?

Table 1. Comparisons between radial velocity method to other planetary observation methods, including transit and microlensing.

Radial Velocity (RV)	Other Methods
• **Distance independent**, tolerate a distance of 160 light years away from the Earth. • No limitations for star-planet position. • Allow direct eccentricity measurement of planet's orbit. • High requirements for signal-to-noise ratio.	**Transit**: • Planet's orbit needs perfectly alignment from the astronomers' vantage point. • Non-repeatable **Microlensing**: • Planetary deviations in light curve are short-lived. • Perfect-timing dependent.

II. Radial Velocity (RV)

- Doppler Effect (blueshift & redshift) due to the gravitational forces between star and planet.
- Planet mass can be calculated from star velocity, as *Eq. 1* derived from Kepler's 3rd law and conservation of momentum.

(Eq. 1)
$$m_p = \frac{m_s V_s}{V_p} = \frac{m_s V_s T}{2\pi r}$$

- Current RV (0.8 m/s) → my last year's new RV (**0.3 m/s**) → goal RV (**0.1 m/s**) [5]

Why so difficult? How to improve?

III. Causes of Imprecise Observation

- Presence of stellar active regions → astrophysical noise in RV time series on rotating stars & intrinsic variations caused by magnetic regions. [6]-[8]
  - Atmospheric turbulence effect → light flux uniformity and wobbles.
  - Absence of useful observations → low planet detectability.
  - RV jitter that mimics planetary signals → obscure transiting planet confirmation.
    - Current lowest RV jitter is **0.45 m/s**, measured from Tau Ceti [9]

PURPOSE

I. Identify the effect of reduced RV error in exoplanet mass detections around K, G, and F dwarf.

II. Identify factors that improve the detectability of planets in habitable zone around K dwarf with improved RV error (0.3 m/s).

- Doubling data points collected, enlarging RV semi-amplitude, and reducing RV jitter.

METHOD I: Mass-Period Plot

I. Mass-Period plot was simulated with reference of *Eq.2* by Gaudi and Winn (2007) [10] (G=Newton' s gravitational constant; P=period; m=planet mass; M=stellar mass; I=orbital inclination with respect to the sky plane; K=RV amplitude):

(Eq. 2)
$$K = \left(\frac{2\pi G}{P}\right)^{\frac{1}{3}} \frac{m \sin I}{(m_s + m_p)^{\frac{2}{3}}}$$

II. HZ calculation from Kepler's 3rd law:

- K dwarf HZ: 0.4-0.6 AU → planet period in HZ: 114.53-210.4 days
- G dwarf HZ: 0.8-1.2 AU → planet period in HZ: 300.00-430 days
- F dwarf HZ: 2.0-2.2 AU → planet period in HZ: 872.52-1006.61 days

III. Compare detectable exoplanet mass for RV precision: **0.3 m/s** (improved) v.s. **0.8 m/s** (previous)

RESULT & DISCUSSION I: Detectable Planet Mass

Mass-Period Plot Simulation: Compare detectable planet mass around K, G, and F Dwarfs.

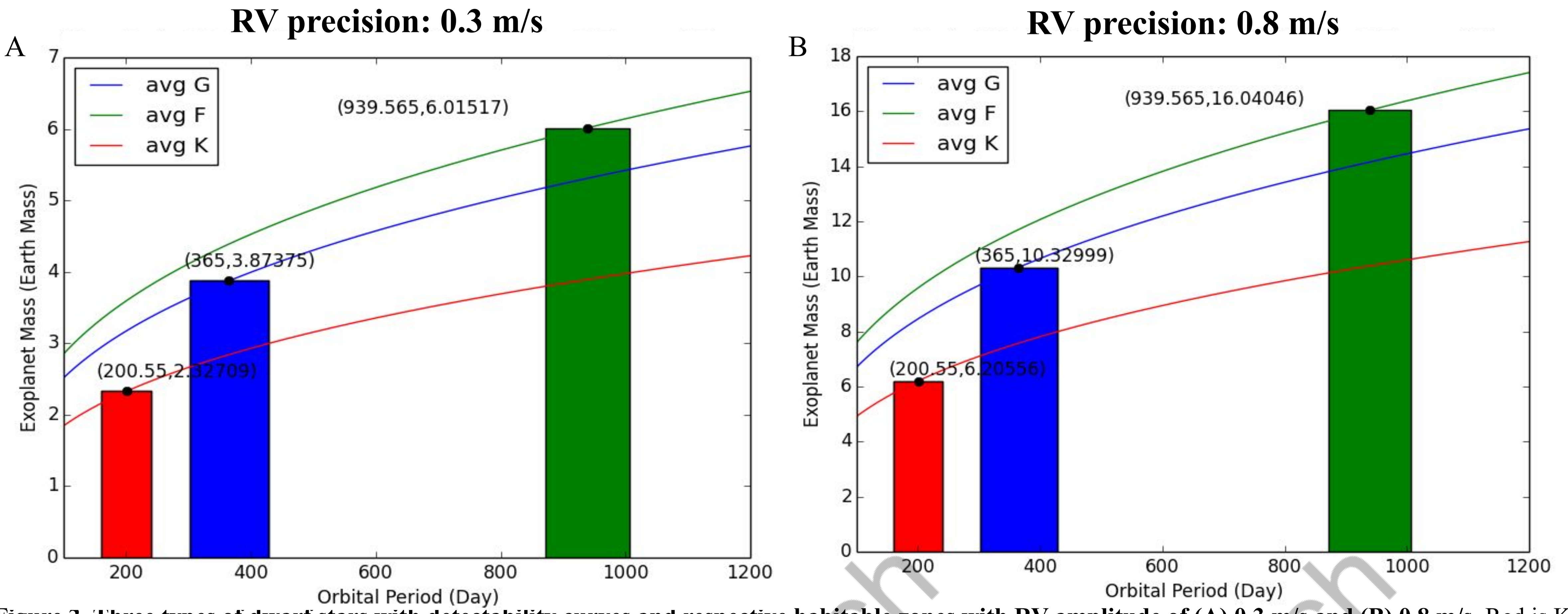

Figure 2. Three types of dwarf stars with detectability curves and respective habitable zones with RV amplitude of (A) 0.3 m/s and (B) 0.8 m/s. Red is K dwarf, blue is G dwarf, and green is F dwarf. Due to the largest mass, F dwarfs have greatest periods. Plots were simulated using python algorithm. The habitable zone was derived from Kopparapu et al., 2013.

Reductions in RV errors (0.3 m/s) permits observations of exoplanets with approximately Earth mass around nearby stars.

0.3 m/s RV precision K,G,F Dwarf detection:

- ~ 2 times Earth-mass planet around K dwarf;
- ~ 3 times around G dwarf;
- ~ 6 times around F dwarf;
- 0.3 m/s RV enables detections of **2-6** times Earth-mass exoplanets

0.8 m/s RV precision K,G,F Dwarf detection:

- ~ 6 times Earth-mass planet around K dwarf;
- ~ 10 times around G dwarf;
- ~ 16 times around F dwarf;
- 0.8 m/s RV enables detections of **6-16** times Earth-mass exoplanets

High Precision Doppler Detections of Nearby Earth-like Exoplanets Assisted by A Double Scrambler

METHOD II: RV Curve Simulations

I. Lomb-scargle periodograms (LS periodogram): designed for unevenly spaced & periodic data simulation [11][12]

II. Variables:
- The number of data points collected.
- RV semi-amplitude changes
  - **0.3 m/s** v.s. **0.6 m/s** → detectable exo-Earth v.s. Super Earth
- RV jitter variations
  - **0.45 m/s** v.s. **0 m/s** → current RV jitter v.s. ideal total jitter removal

III. Successful detections are characterized as:
- Falls in the range of mid HZ ± 10% mid HZ
- The dominant peak on LS periodogram overlaps the mid HZ line.

IV. Data analysis:
- A python algorithm was written to simulate the LS periodograms with variables: eccentricity (0), instrument RV (0.3 m/s), argument of periapsis (90), **RV jitter (0.45 m/s or 0 m/s), period (depends on stars), number of data points (100 or 200), RV amplitude (0.3 m/s or 0.6 m/s).**

RESULT & DISCUSSION II: Planet Period Simulation

I. **K, G, F Dwarf Periodogram Simulation:** Determine planet distance from the host star by observing orbit period and dominant peak.

K Dwarf

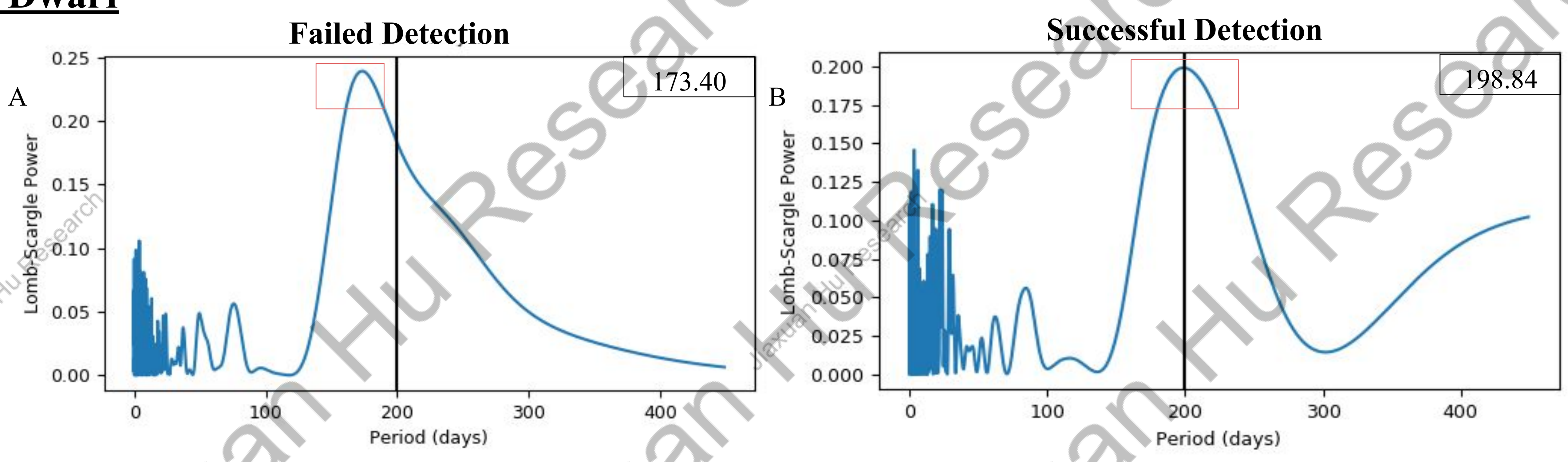

Figure 3. Lomb-Scargle Periodogram simulated for K Dwarf in a period of 200 days. Radial velocity error was 0.3 m/s, RV jitter was 0.45 m/s, and 100 data plots were simulated using rv_simulation.py algorithm. (A) is failed detection that the output period was not in a range of 180-220 days. (B) is successful detection, and the dominant peak was approximately on the 200 days line.

- Successful detection: planet period falls in the range of 180~220 days.
- Failed detection period of 173. 40 days (Fig. 3A) → planets orbiting too close to the host star.
- Successful detection period of 198.84 days (Fig. 3B) → planets orbiting in HZ.

G Dwarf

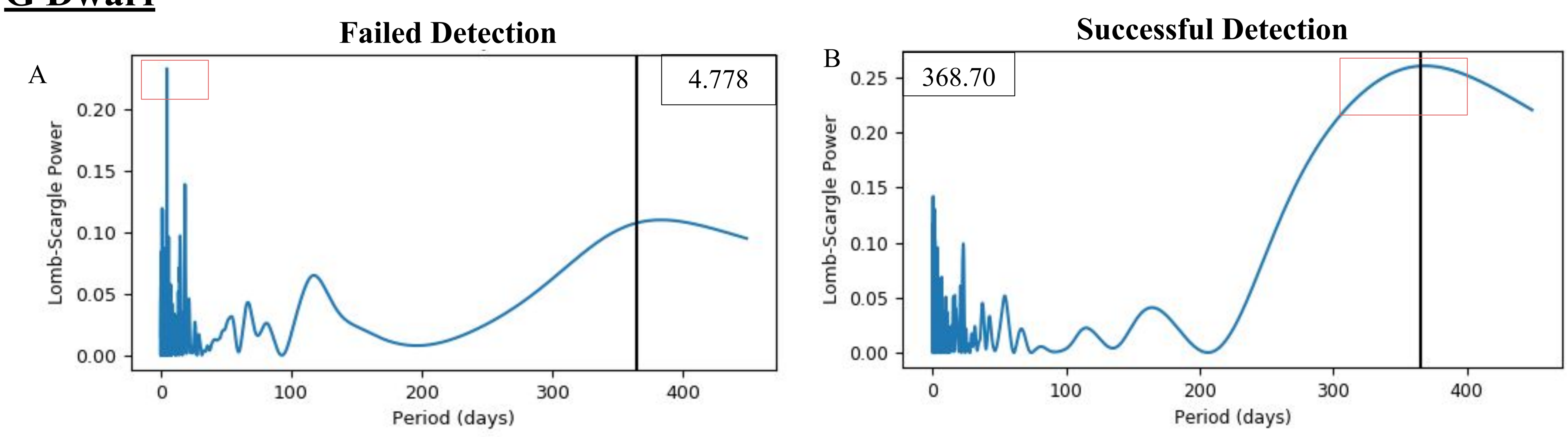

Figure 4. Lomb-Scargle Periodogram simulated for G Dwarf in a period of 365 days. Radial velocity error was 0.3 m/s, RV jitter was 0.45 m/s, and 100 data plots were simulated using rv_simulation.py algorithm. (A) failed detections that the output periods were not in a range of 328.5-401.5 days. (B) successful detections and their dominant peaks were approximately on the 365 days line.

- Successful detection falls in the period of 328.5-401.5 days.
- Failed detection period of 4.778 days (Fig. 4A) → planets orbiting too close to the host star.
- Successful detection period of 368.70 days (Fig. 4B) → planets orbiting in HZ.

F Dwarf

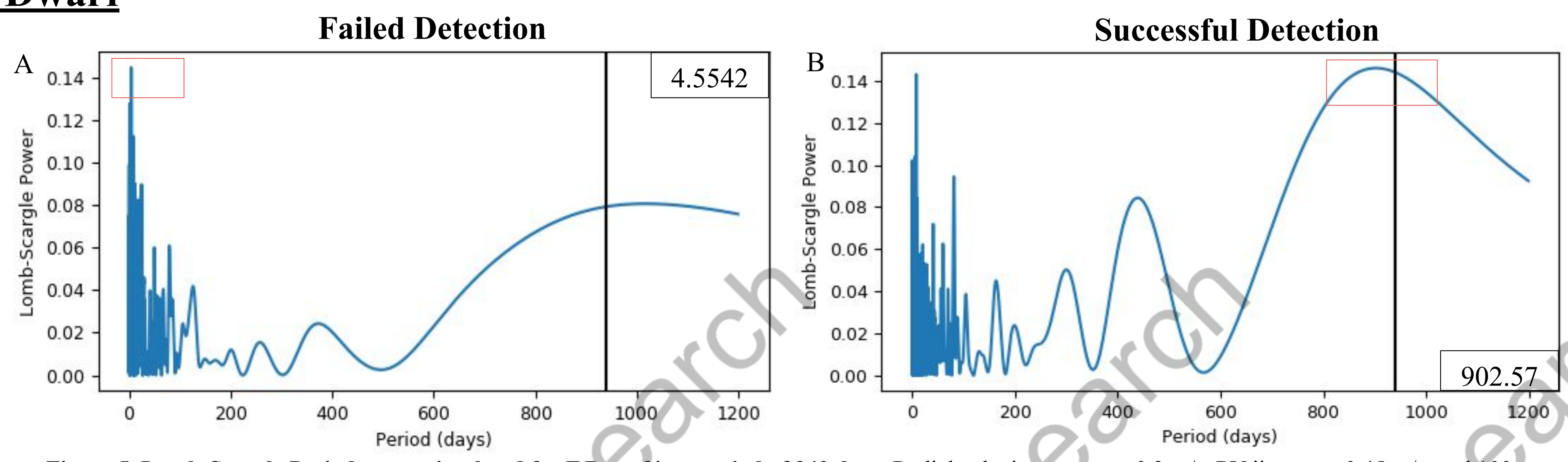

Figure 5. Lomb-Scargle Periodogram simulated for F Dwarf in a period of 940 days. Radial velocity error was 0.3 m/s, RV jitter was 0.45 m/s, and 100 data plots were simulated using rv_simulation.py algorithm. (A) failed detections that the output periods were not in a range of 854.1-1043.9 days. (B) successful detections and their dominant peaks were approximately on the 940 days line.

- Successful detection falls in the period of 854.1-1043.9 days.
- Failed detection period of 4.5542 days (Fig. 5A) → planets orbiting too close to the host star.
- Successful detection period of 902.57 days (Fig. 5B) → planets orbiting in HZ.

RESULT & DISCUSSION II: Planet Orbit (cont.)

II. Detectability Improvement Around K Dwarf: Determine factors that can enhance planet detectability in HZ.

RV jitter: 0.45 m/s

Table 2. 100 simulated RV successful detections in the K dwarf habitable zone with RV jitter of 0.45 m/s. When target exoplanet mass (RV amplitude limit) or data plots increase, the percentages of successful detections also increase. 0.3 m/s RV amplitude with 100 data points is the control group. Successful detections were simulated using a python algorithm.

	Trial 1	Trial 2	Trial 3	Mean	Standard Dev.
0.3 m/s; 100 data points	20%	19%	16%	18.3%	8.1%
0.3 m/s; **200** data points	47%	55%	46%	49.3%	4.0%
0.6 m/s; 100 data points	31%	35%	36%	34.0%	2.2%

- Highest detectability of 49.3% when observing with 0.3 m/s semi-amplitude & 200 data points. (Table 2)
- Increase data points and RV amplitude result in enhanced detectability.
  - Increase data points allow more useful observations.
  - Increase RV amplitude allow larger mass exoplanets as targets in observations.

RV jitter: 0 m/s (ideal cases)

Table 3. 100 simulated RV successful detections in the K dwarf habitable zone with RV jitter of 0 m/s. When target exoplanet mass (RV amplitude limit) or data plots increase, the percentages of successful detections also increase. The 0.3 m/s RV amplitude with 100 data points is the control group.

	Trial 1	Trial 2	Trial 3	Mean	Standard Dev.
0.3 m/s; 100 data points	49%	49%	49%	49.0%	0.0%
0.3 m/s; **200** data points	52%	55%	67%	58%	6.5%
0.6 m/s; 100 data points	71%	72%	71%	71.3%	0.1%
0.6 m/s; **200** data points	82%	86%	80%	82.7%	2.5%

- Highest detectability of **82.7%** when observing with 0.6 m/s semi-amplitude & 200 data points. (Table 3)
- Every variable indicates an increase in detectability, so total removal of RV jitter improve exoplanet detections in HZ around K dwarf.

CONCLUSION

I. The 0.3 m/s RV error enables the detection of **2-6** times Earth-mass exoplanets around K, G, and F dwarfs, a significant improvement compared with previous 0.8 m/s.

II. Doubling data points collected, enlarging RV semi-amplitude, and removing RV jitter allow a higher detectability of planets in HZ around K dwarf.

a. Doubling data points depend on weather conditions, air quality, and seasons for observation.
b. Enlarging RV semi-amplitude lack feasibility because it only opens the tolerance of Earth-mass planets.
c. Reducing RV jitter is the most expedient method to lessen the effect of intrinsic variations on the observation.

FUTURE INVESTIGATION

I. A double scrambler should be improved to 2-3 times precision to reduce RV errors from current 0.2-0.3 m/s. [15]

II. Factors such as guiding errors and tip-tilt errors can be considered to enhance fiber optics light flux stability and uniformity.[14]-[16]
- Guiding errors: inevitable, but can be reduced to a minimum with the correct guiding hardware.
- Tip-tilt errors: can be addressed by improving lenses and focal plane.

III. Careful selection of seasons and weathers for observation can enhance the successful rate to locate planets in HZ.[17]

IV. Long exposures of images taken can reduce the influence of stellar oscillations on RV jitter.[7][18][19]

V. The RV error needs to be reduced to ~0.1 m/s for detections of **0.7~2** times Earth-mass exoplanets. (Fig. 6) [13][14]

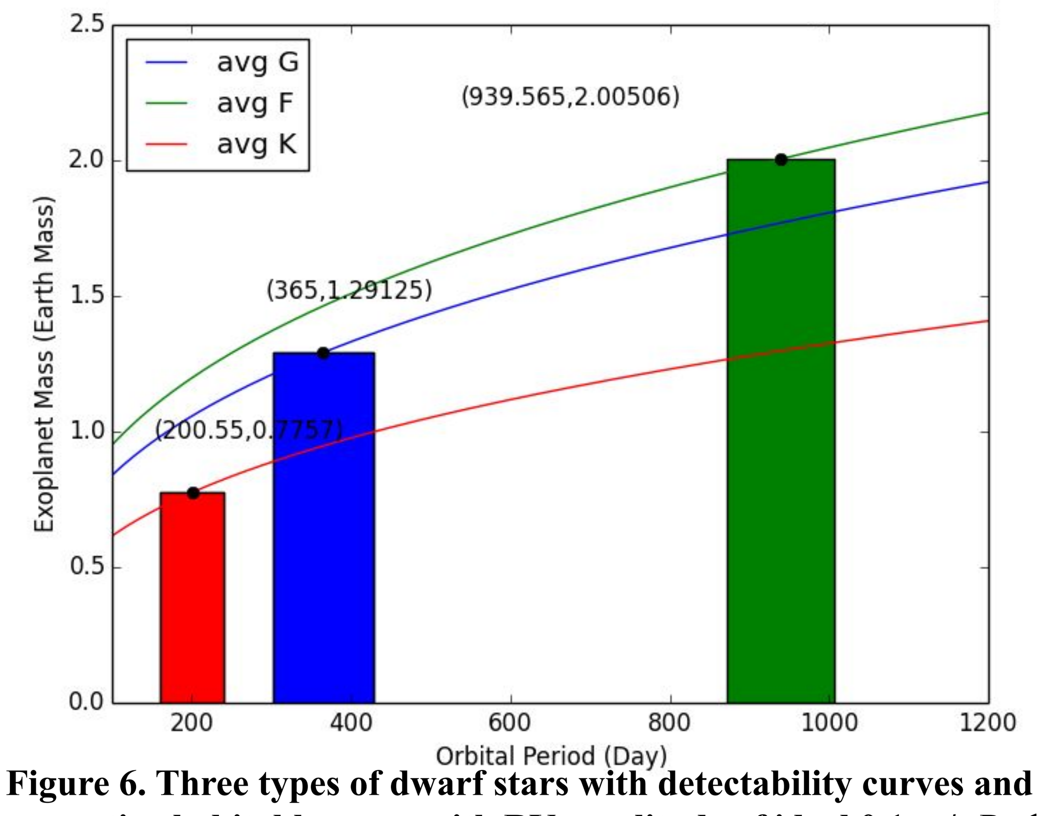

Figure 6. Three types of dwarf stars with detectability curves and respective habitable zones with RV amplitude of ideal 0.1 m/s Red is K dwarf, blue is G dwarf, and green is F dwarf.

REFERENCE

[1] G. Torres, S. R. Kane, J. F. Rowe, N. M. Batalha, C. E. Henze, D. R. Ciardi, T. Barclay, W. J. Borucki, L. A. Buchhave, J. R. Crepp, M. E. Everett, E. P. Horch, A. W. Howard, S. B. Howell, H. T. Isaacson, J. M. Jenkins, D. W. Latham, E. A. Petigura, and E. V. Quintana, "Validation of Small Kepler Transiting Planet Candidates in or near the Habitable Zone," The Astronomical Journal, vol. 154, no. 6, p. 264, 2017.
[2] A. S. Mascareño, R. Rebolo, J. I. G. Hernández, and M. Esposito, "Characterization of the radial velocity signal induced by rotation in late-type dwarfs," Monthly Notices of the Royal Astronomical Society, vol. 468, no. 4, pp. 4772–4781, 2017.
[3] G. Fűrész, R. Pawluczyk, P. Fournier, R. Simcoe, and D. F. Woods, "Pupil slicer design for the NASA-NSF extreme precision Doppler spectrograph concept WISDOM," Advances in Optical and Mechanical Technologies for Telescopes and Instrumentation II, 2016.
[4] N. Batalha and W. Stenzel, "Kepler's Small Habitable Zone Planets," NASA, 08-Dec-2016. [Online]. Available: https://www.nasa.gov/mission_pages/kepler/multimedia/images/keplers-small-habitable-zone-planets.
[5] M. Johnson, "How many exoplanets has Kepler discovered?," NASA, 09-Apr-2015. [Online]. Available: https://www.nasa.gov/kepler/discoveries/. [Accessed: 14-Nov-2018].
[6] F. Bouchy, R. F. Díaz, G. Hébrard, L. Arnold, I. Boisse, X. Delfosse, S. Perruchot, and A. Santerne, "SOPHIE+: First results of an octagonal-section fiber for high-precision radial velocity measurements," Astronomy & Astrophysics, vol. 549, 2012.
[7] D. A. Fischer, G. Anglada-Escude, P. Arriagada, R. V. Baluev, J. L. Bean, F. Bouchy, J. T. Wright, "State of the field: extreme precision radial velocities," Publications of the Astronomical Society of Pacific, vol. 128, no. 964, 2016.
[8] B. Ma, J. Ge, "Data reduction pipeline of the TOU optical very high resolution spectrograph and its sub-m/s performance," MNRAS, pp. 1-12, 2018.
[9] I. Gris-Sánchez, D. M. Haynes, K. Ehrlich, R. Haynes, and T. A. Birks, "Multicore fibre photonic lanterns for precision radial velocity science," Monthly Notices of the Royal Astronomical Society, 2017.
[10] B. S. Gaudi and J. N. Winn, "Prospects for the Characterization and Confirmation of Transiting Exoplanets via the Rossiter‐McLaughlin Effect," The Astrophysical Journal, vol. 655, no. 1, pp. 550–563, 2007.[11] S. Halverson, A. Roy, S. Mahadevan, L. Ramsey, E. Levi, C. Schwab, F. Hearty, and N. Macdonald, "An Efficient, Compact, And Versatile Fiber Double Scrambler For High Precision Radial Velocity Instruments," The Astrophysical Journal, vol. 806, no. 1, p. 61, Sep. 2015.
[11] J. T. Vanderplas, "Understanding the Lomb–Scargle Periodogram," The Astrophysical Journal Supplement Series, vol. 236, no. 1, p. 16, Nov. 2018.
[12] D. Queloz, G. W. Henry, J. P. Sivan, S. L. Baliunas, J. L. Beuzit, R. A. Donahue, M. Mayor, D. Naef, C. Perrier, and S. Udry, "No planet for HD 166435," Astronomy and Astrophysics, vol. 379, no. 1, pp. 279–287, 2001.
[13] N. C. Santos, A. Mortier, J. P. Faria, X. Dumusque, V. Z. Adibekyan, E. Delgado-Mena, P. Figueira, L. Benamati, I. Boisse, D. Cunha, J. G. D. Silva, G. L. Curto, C. Lovis, J. H. C. Martins, M. Mayor, C. Melo, M. Oshagh, F. Pepe, D. Queloz, A. Santerne, D. Ségransan, A. Sozzetti, S. G. Sousa, and S. Udry, "The HARPS search for southern extra-solar planets," Astronomy & Astrophysics, vol. 566, 2014.
[14] N. Huélamo, P. Figueira, X. Bonfils, N. C. Santos, F. Pepe, M. Gillon, R. Azevedo, T. Barman, M. Fernández, E. D. Folco, E. W. Guenther, C. Lovis, C. H. F. Melo, D. Queloz, and S. Udry, "TW Hydrae: evidence of stellar spots instead of a Hot Jupiter," Astronomy & Astrophysics, vol. 489, no. 2, 2008.
[15] P. Plavchan, D. Latham, S. Gaudi, J. Crepp, X. Dumusque, G. Furesz, A. Vanderburg, C. Blake, D. Fischer, L. Prato, R. White, V. Makarov, G. Marcy, K. Stapelfeldt, R. Haywood, A. Collier-Cameron, A. Quirrenbach, S. Mahadevan, G. Anglada, P. Muirhead, "Radial Velocity Prospects Current and Future: A White Paper Report prepared by the Study Analysis Group 8 for the Exoplanet Program Analysis Group (ExoPAG)," Instrumentation and Methods for Astrophysics, 2015.
[16] J. T. Wright, "Radial Velocity Jitter in Stars from the California and Carnegie Planet Search at Keck Observatory," Publications of the Astronomical Society of the Pacific, vol. 117, no. 833, pp. 657–664, 2005.
[17] I. Boisse, F. Bouchy, B. Chazelas, S. Perruchot, F. Pepe, C. Lovis, and G. Hébrard, "Consequences of spectrograph illumination for the accuracy of radial-velocimetry," EPJ Web of Conferences, vol. 16, p. 02003, 2011.
[18] H. Isaacson and D. Fischer, "Chromospheric Activity And Jitter Measurements For 2630 Stars On The California Planet Search," The Astrophysical Journal, vol. 725, no. 1, pp. 875–885, 2010.
[19] R. Martínez-Arnáiz, J. Maldonado, D. Montes, C. Eiroa, and B. Montesinos, "Chromospheric activity and rotation of FGK stars in the solar vicinity," Astronomy and Astrophysics, vol. 520, 2010.